



ISTITUTO NAZIONALE DI RICERCA METROLOGICA Repository Istituzionale

Spectral super-resolution spectroscopy using a random laser

This is the author's accepted version of the contribution published as:

Original

Spectral super-resolution spectroscopy using a random laser / Boschetti, Alice; Taschin, Andrea; Bartolini, Paolo; Tiwari, Anjani Kumar; Pattelli, Lorenzo; Torre, Renato; Wiersma, Diederik S.. - In: NATURE PHOTONICS. - ISSN 1749-4885. - 14:3(2020), pp. 177-182. [10.1038/s41566-019-0558-4]

Availability:

This version is available at: 11696/60967 since: 2020-05-26T20:39:15Z

Publisher:

Springer

Published

DOI:10.1038/s41566-019-0558-4

Terms of use:

This article is made available under terms and conditions as specified in the corresponding bibliographic description in the repository

Publisher copyright

(Article begins on next page)

Spectral super-resolution spectroscopy using a random laser

Alice Boschetti^{*1}, Andrea Taschin^{1,2}, Paolo Bartolini¹, Anjani Kumar Tiwari³, Lorenzo Pattelli^{1,4},
Renato Torre^{1,5}, Diederik S. Wiersma^{*1,4,5}

¹European Laboratory for Non-Linear Spectroscopy (LENS) / University of Florence, Via Nello Carrara, 1 -
50019 Sesto Fiorentino, Italia

²ENEA, Centro Ricerche Frascati, Via E. Fermi, 45 – 00044, Frascati, Italia

³Department of Physics, Indian Institute of Technology Kanpur, 208016 Kanpur, India

⁴Istituto Nazionale di Ricerca Metrologica (INRIM), Strada delle Cacce, 91 – 10135 Torino, Italia

⁵Department of Physics, University of Florence, Via Sansone, 1 – 50019 Sesto Fiorentino, Italia

*email: boschetti@lens.unifi.it, wiersma@lens.unifi.it

Abstract

Super-resolution microscopy refers to a powerful set of imaging techniques that overcome the diffraction limit. Some of these techniques, of which the importance was emphasized by the 2014 Nobel Prize for chemistry, are based on the clever concept of image reconstruction by spatially sparse sampling. Here, we introduce the concept of super-resolution spectroscopy based on sparse sampling in the frequency domain, and show that this can be naturally achieved using a random laser source. In its chaotic regime, the emission spectrum of a random laser features sharp spikes at uncorrelated frequencies that are sparsely distributed over the emission bandwidth. These narrow lasing modes probe stochastically the spectral response of a sample, allowing to

33 reconstruct it with a resolution exceeding that of the spectrometer. We envision that
34 the proposed technique will inspire a new generation of simple and cheap, high-
35 resolution spectroscopy tools with reduced footprint.

36

37 In general, the concept of super-resolution refers to the possibility to obtain a higher quality digital
38 reconstruction of a detected signal, using sets of low-resolution measurements. In the field of optics, various
39 methods have been proposed for super-resolution imaging, with the aim of obtaining a resolution that is
40 beyond the diffraction limit^{1,2,3,4,5}. Super-resolution microscopy based on single molecule localization has
41 undergone a rapid development in recent years^{6,7,8}. It relies on the principle of repetitive and spatially sparse
42 activation of point-like sources inside the sample. Each point source generates a blurred disk-shape whose
43 centroid can be obtained with sub-pixel resolution by a fitting procedure. While one image only contains the
44 information on a few points of the desired object, accumulating a large amount of such points allows to
45 reconstruct the entire image at a resolution that is much higher than that of the imaging system.

46 Some attempts have been undertaken to improve the resolution of spectral measurements, for instance,
47 by making use of known information regarding the source. Out of these, a few noteworthy approaches include
48 the analysis of spectra that can be assumed to have a compact representation⁹ or the extension of a dataset in
49 the Fourier domain to improve resolution of the target signal¹⁰.

50 In this work, we wish to introduce a new idea in spectroscopy, namely that of sparse sampling in the
51 frequency domain, using random lasers as light source. The purpose is to achieve super-resolution in the
52 spectroscopic characterization of samples; that is, to obtain a characterization with spectral features that are
53 finer than the nominal resolution of the spectrometer. Below we will explain the idea and discuss various
54 aspects of its implementation. We will start with a numerical simulation to test the concept and then show an
55 experimental realization where the spectrum of a custom-made etalon filter is reconstructed as an example.

56 It is well-known that the resolution of a spectrometer can be defined by the Rayleigh criterion¹¹ i.e., its
57 ability to identify two adjacent spectral lines. This is strictly connected with the spectral “instrumental line
58 profile”, $I(\lambda)$, corresponding to the spectral line measured by a detector at the output slit if a “monochromatic
59 field” is focused at the spectrometer entrance slit. The full width half maximum (FWHM) of $I(\lambda)$ defines the

60 spectrometer resolution. This implies that any spectrum $S(\lambda)$, analysed by the spectrometer, is the result of the
61 convolution of the real spectrum $S_0(\lambda)$ with the instrumental line profile $I(\lambda)$:

$$62 \quad S(\lambda) = S_0(\lambda) \otimes I(\lambda). \quad [\text{eq.1}]$$

63 The shape of $I(\lambda)$ depends both on the properties of the spectrometer and the detector.

64 To explore the possibility of using a random laser source for super-resolution spectroscopy, let us consider
65 the example of a low-finesse Fabry Perot (FP) characterized by a free spectral range (FSR) well below the
66 spectral resolution of a measuring apparatus (FWHM = $4.9 \times \text{FSR}$). We will first consider a numerical simulation
67 of this system and later in the paper report on its experimental characterization, using, in both cases, the
68 concept of sparse sampling in the spectral domain with a random laser as light source.

69 **A numeric example**

70 In Figure 1, the outline of the setup is shown as modelled in the numerical simulation. This outline also
71 serves to illustrate the idea more in detail. Two types of light sources have been considered: a random laser
72 (blue in the figure) and a regular lamp as comparison (yellow in the figure). The transmission of the etalon is
73 measured versus frequency, using a low resolution spectrometer (indicated in green, together with its (broad)
74 spectral response function). In the yellow graph (panel b) the optical response is shown when the sample is
75 illuminated with an ideal Gaussian-shaped broadband illumination source. Due to the convolution of the
76 transmission spectrum of the sample with the (broad) instrumental response function of the spectrometer, the
77 Fabry-Perot fringes disappear almost completely. From a mathematical point of view, by knowing $I(\lambda)$ exactly
78 for an ideal delta-like source, it would still be possible to recover the original signal using a deconvolution
79 operation. However, this is unfeasible in practice due to the finite noise level of any real measurement, and it
80 is in fact already challenging even in this simulated case due to numerical instability of deconvolution, which is
81 highly susceptible to finite precision of computed functions^{12,13}.

82 Here, we will show that it is possible to retrieve the target transmission function by performing a sparse
83 frequency sampling, just as sparse spatial sampling allows to retrieve an image in super-resolution microscopy.
84 More precisely, we will use a random laser in the chaotic regime as the illumination source, taking advantage
85 of the inherent spectral separation of a typical random laser emission spectrum. Random lasers are laser

86 sources using a disordered gain medium, with no external cavity^{14,15}. The term ‘random lasing’ refers to the
87 fact that its modes are disordered in nature. The physics behind random lasing is quite rich^{14,16}. For instance,
88 the number of modes is typically huge and a large amount of modes can be overlapping both in space and
89 frequency. This leads to strong mode coupling and a broad parameter regime in which the output is chaotic¹⁷.
90 At each random laser shot only a few modes actually reach threshold leading to the typical random laser
91 emission spectrum that consist of a few narrow ‘spikes’ well-separated from each other. Additionally, in the
92 chaotic regime of operation, the emission spectrum of each random laser pulse is completely uncorrelated
93 from the previous pulse. Overall, these properties make random lasers an ideal class of sources for sparse
94 sampling in the frequency domain.

95 By recording peak amplitudes and frequencies for the most prominent peaks through a series of chaotic
96 spectra, it is possible to reconstruct the super-resolved transmission function of a sample with its original
97 contrast. Typically, having only a few prominent peaks for each lasing spectrum, it is possible to retrieve their
98 centre frequency with high, sub-pixel precision. Once a large ensemble (in the order of a few thousand
99 depending on the desired level of signal-to-noise ratio) of lasing peaks has been collected, plotting their
100 amplitudes as a function of frequency provides a reconstruction of the super-resolved target spectrum, free of
101 deconvolution artefacts.

102 Numerical simulations have been performed on large sets of computer generated random laser spectra to
103 test the concept and to understand its ideal parameters of operation (including the number of lasing modes,
104 their optimal spacing, and the number of spectra over which one should average). In Figure 1d, a few of the
105 numerically simulated transmission spectra have been plotted. In each transmission curve, one can identify
106 isolated broadened peaks of which the centre can be identified. Each of such peaks then provides one point in
107 the reconstruction of the target spectrum. In the bottom panel of Figure 1, the reconstructed spectrum is
108 shown using a total of 10^4 single shot random laser spectra with a simulated noise level of 0.1% of the
109 maximum of the fluorescence curve. For comparison, we also show the result for a broadband source like a
110 regular lamp, using the same parameters. While nearly all information is lost using the broadband source,
111 random laser illumination allows to reconstruct the target spectrum with very good precision. Regular
112 deconvolution is very sensitive to small noise fluctuations – which are amplified in the reconstructed spectrum.
113 The statistical reconstruction using a random laser is much more stable and successfully retrieves the original

114 Fabry-Perot contrast and spectral pattern – especially in the central region where the random laser statistics is
115 larger. We have performed a broad range of similar simulations and found that random laser based super-
116 resolved spectral reconstruction can be applied nearly arbitrarily, for a wide range of apparatus response
117 functions and target transmission spectra.

118 **Experimental results**

119 In order to test our ideas in practice, we performed an experimental analysis, again using a Fabry-Perot as
120 an example. The etalon was realized with a free spectral range of 0.3 THz and a maximum transmission
121 contrast of 32%. A spectrometer was used with a resolution that did not allow to resolve the interference
122 fringes of the etalon (FWHM= 2.8·FSR). The analysis was performed with a random laser and with a regular
123 lamp for comparison. The outline of the experimental setup is sketched in Figure 2. A microscope objective is
124 used both to focus the pump laser and to collect the random laser signal. The random laser emission is split by
125 a 50:50 beam splitter into two beams: a reference signal – which is directly coupled to one entrance of a
126 multimodal fibre bundle, and a probe signal passing through the sample before being focused on the other
127 fibre entrance. A magnified image of the two fibre ends is reproduced on the entrance slit of a
128 monochromator, and a CCD camera finally records the image reproduced on its output focal plane. (See
129 Methods section for more details.)

130 The random laser was realized by suspending ZnO nanoparticles in a solution of Rhodamine 6G and ethanol
131 (see Methods for technical details). A frequency doubled Nd:YAG laser was used to optically pump the random
132 laser. Lasing was observed above a threshold of 0.5 μJ energy per pump pulse. The laser was operated above
133 threshold but still well within its chaotic regime of operation, characterized by Lévy-distributed intensity
134 fluctuations^{18,19}. Single-shot emission spectra are found to be entirely uncorrelated, with narrow peaks
135 appearing at independent frequencies. An example of such an emission spectrum is shown in Figure 2b, while
136 more examples can be found in the supplementary information. The output of this random laser was then
137 used as a source to characterize the FP, whose transmission function is shown in Figure 2c as measured
138 independently with a high-resolution spectrometer with a linewidth 0.13 THz.

139 Figure 2d reports the transmission spectrum of a single random laser shot as measured by the low-
140 resolution spectrometer. The sample modulates the intensity of the probe signal with respect to the reference,

141 but, as expected, the visibility of the FP transfer function is completely lost even in the fluorescence
142 background. Nonetheless, information on the transmission function of the sample is still contained in the
143 relative heights of the peaks in the measured spectrum and can be retrieved by analysing a large number of
144 random laser shots. For that purpose, the centre of each peak should be determined accurately, as well as the
145 modulation of the peak height by the sample (obtained by comparing the transmission through the sample
146 with the reference beam).

147 The steps of this statistical analysis are shown in Figure 3. A set of 4000 single-shot random laser spectra is
148 collected, each of them producing a double trace. All traces contain both the transmitted signal (bottom) as
149 well as its respective reference signal (top). For each shot, isolated random laser modes are selected by an
150 algorithm that identifies bright disks within a certain diameter range as defined by the spectral resolution of
151 the spectrometer. For each disk selected in the transmission signal, we compute its intensity by integrating
152 over the disk area and normalizing it by the integral of the respective disk found in the reference signal. The
153 reference signal is also used to determine the central frequency of the unaltered peak in order to avoid
154 apparent frequency shifts that could be possibly induced by steep modulations of the transmission function.

155 **Discussion**

156 The procedure of sparse sampling in the frequency domain allows to reconstruct the transmission function of
157 the sample. We should note here that by “sparse sampling” we simply refer to a minimum average spectral
158 separation between the lasing peaks. Seeking this condition is an important factor for the efficiency of the
159 reconstruction technique as it can reduce drastically the probability of having two almost-degenerate lasing
160 modes during the same laser shot, which would go unresolved by the spectrometer (See SI). Frequency
161 sparsity is an intrinsic characteristic of random laser emission spectra and it can be exploited to achieve a
162 sampling of a transmission function unaffected from convolution effects. By acquiring a sufficiently large
163 statistics on the transmitted frequency positions and amplitudes, the whole spectrum can be reconstructed, as
164 we show for our exemplary test case in Figure 4a.

165 One can clearly see that the transmission function of the FP etalon is reconstructed with all its relevant
166 features. For comparison, when the transmission spectrum is measured using a standard lamp as light source,
167 the etalon transmission function cannot be retrieved even when averaging over the same amount of spectra to

168 reduce measurement noise (Fig. 4b). The effectiveness of the method is further highlighted by analysing the
169 results in the Fourier domain. The periodicity of the transmission function of the FP etalon is clearly retrieved
170 when using the random laser, while it is lost in the lamp measurements (See Figs. 4c and 4d).

171 In conclusion, we have shown that it is possible to perform super-resolution *spectroscopy* exploiting the
172 intrinsic features of random laser emission for spectral sparse sampling – analogously to sparse sampling in
173 super-resolution *microscopy*. We have introduced the idea, analysed its parameter space of operation using
174 numerical calculations, and performed an experimental demonstration on a test etalon sample. Our results
175 show that it is possible to retrieve spectral features of a transfer function below the resolution limit imposed
176 by the spectrometer. As confirmed by our analysis both in direct and reciprocal space, our method delivers
177 accurate reconstruction despite minimal algorithm optimization and the moderate size of the statistical
178 ensemble of random laser peaks used.

179 We have shown a ~ 3 spectral enhancement factor, but in principle the method can be adapted to
180 spectrometers whose response function is arbitrary in width and shape, which poses no upper limit to the
181 effective enhancement that can be achieved. In absolute terms, an ultimate resolution limit is represented by
182 the linewidth of the individual random laser modes (which, in our case, was around 0.19 THz). Random lasing
183 modes with much narrower widths can be obtained, e.g., by spatially tailoring the pumping light²⁰.
184 Additionally, compressive sensing methods should be straightforwardly applicable to the reconstruction
185 technique in order to reduce the number of spectra required to obtain a certain signal-to-noise level^{21,22}.

186 Most importantly, our approach relies entirely on the chaotic variation of the illumination spectrum to ensure
187 narrow line widths and a uniform sampling over the emission band, and hence does not require any
188 stabilization of the lasing source – which is otherwise critical in other high-resolution approaches such as
189 frequency comb spectroscopy²³, nor it requires an exact knowledge of the instrumental spectral response as
190 in typical deconvolution algorithms.

191 Quite interesting, the distinctive features of random laser emission – namely their huge variety of modes, their
192 chaotic behaviour and naturally sparse population – make these illumination sources ideal candidates for this
193 super-resolved stochastic reconstruction approach. We believe that the concept introduced in this paper can
194 possibly lead to a new generation of high-resolution spectral analysis providing a small footprint, low-cost

195 alternative to the use of more expensive broadband-tunable narrow line lasers. Our technique is based on a
196 general principle and can be straightforwardly replicated in different wavelength regions ranging from the UV
197 to the mid-infrared, where random laser sources are already available^{24,25,26,27,28,29}. Taking advantage of more
198 recent electrically-pumped random lasing schemes holds promise to further extend the applicability of our
199 approach, making it making it more energy-efficient, compatible with CMOS technology and suitable for large-
200 scale production and integration in devices^{30,31}.

201

202 **Data availability**

203 The data that support the plots within this paper and other findings of this study are available from the
204 corresponding author upon reasonable request.

205

206

207

Bibliography

208

- 209 1. Betzig, E., Trautman, J. K., Harris, T. D., Weiner, J. S. & Kostelak, R. L. Breaking the diffraction barrier:
210 optical microscopy on a nanometric scale. *Science* **251**, 1468–70 (1991).
- 211 2. Hell, S. W. & Wichmann, J. Breaking the diffraction resolution limit by stimulated emission: stimulated-
212 emission-depletion fluorescence microscopy. *Opt. Lett.* **19**, 780 (1994).
- 213 3. Gazit, S., Szameit, A., Eldar, Y. C. & Segev, M. Super-resolution and reconstruction of sparse sub-
214 wavelength images. *Opt. Express* **17**, 23920 (2009).
- 215 4. Szameit, A. *et al.* Sparsity-based single-shot subwavelength coherent diffractive imaging. *Nat. Mater.*
216 **11**, 455–459 (2012).
- 217 5. Huang, F. M. & Zheludev, N. I. Super-Resolution without Evanescent Waves. *Nano Lett.* **9**, 1249–1254
218 (2009).
- 219 6. Rust, M. J., Bates, M. & Zhuang, X. Sub-diffraction-limit imaging by stochastic optical reconstruction
220 microscopy (STORM). *Nat. Methods* **3**, 793–796 (2006).
- 221 7. Hess, S. T., Girirajan, T. P. K. & Mason, M. D. Ultra-High Resolution Imaging by Fluorescence
222 Photoactivation Localization Microscopy. *Biophys. J.* **91**, 4258–4272 (2006).

- 223 8. Betzig, E. *et al.* Imaging intracellular fluorescent proteins at nanometer resolution. *Science* **313**, 1642–5
224 (2006).
- 225 9. Kawata, S., Minami, K. & Minami, S. Superresolution of Fourier transform spectroscopy data by the
226 maximum entropy method. *Appl. Opt.* **22**, 3593 (1983).
- 227 10. Sidorenko, P. *et al.* Super-resolution spectroscopy by compact representation. in *Frontiers in Optics*
228 *2012/Laser Science XXVIII FM3F.5* (OSA, 2012). doi:10.1364/FIO.2012.FM3F.5
- 229 11. Pedrotti, F. L., & Pedrotti, L. S. *Introduction to optics*. (Prentice-Hall, 1987).
- 230 12. Blass, W. E. & Halsey, G. W. *Deconvolution of absorption spectra*. (Academic Press, 1981).
- 231 13. Mou-Yan, Z. & Unbehauen, R. A deconvolution method for spectroscopy. *Meas. Sci. Technol.* **6**, 482–
232 487 (1995).
- 233 14. Wiersma, D. S. The physics and applications of random lasers. *Nat. Phys.* **4**, 359–367 (2008).
- 234 15. Liu, J. *et al.* Random nanolasing in the Anderson localized regime. *Nat. Nanotechnol.* **9**, 285–289
235 (2014).
- 236 16. Cao, H., Chriki, R., Bittner, S., Friesem, A. A. & Davidson, N. Complex lasers with controllable
237 coherence. *Nat. Rev. Phys.* **1**, 156–168 (2019).
- 238 17. Uppu, R., Tiwari, A. K. & Mujumdar, S. Identification of statistical regimes and crossovers in coherent
239 random laser emission. *Opt. Lett.* **37**, 662 (2012).
- 240 18. Araújo, C., Gomes, A. & Raposo, E. Lévy Statistics and the Glassy Behavior of Light in Random Fiber
241 Lasers. *Appl. Sci.* **7**, 644 (2017).
- 242 19. Sharma, D., Ramachandran, H. & Kumar, N. Lévy statistics of emission from a novel random amplifying
243 medium: an optical realization of the Arrhenius cascade. *Opt. Lett.* **31**, 1806 (2006).
- 244 20. Bachelard, N., Gigan, S., Noblin, X. & Sebbah, P. Adaptive pumping for spectral control of random
245 lasers. *Nat. Phys.* **10**, 426–431 (2014).
- 246 21. Zhu, L., Zhang, W., Elnatan, D. & Huang, B. Faster STORM using compressed sensing. *Nat. Methods* **9**,
247 721–723 (2012).
- 248 22. Katz, O., Bromberg, Y. & Silberberg, Y. Compressive ghost imaging. *Appl. Phys. Lett.* **95**, 131110 (2009).
- 249 23. Picqué, N. & Hänsch, T. W. Frequency comb spectroscopy. *Nat. Photonics* **13**, 146–157 (2019).
- 250 24. Liang, H. K. *et al.* Electrically Pumped Mid-Infrared Random Lasers. *Adv. Mater.* **25**, 6859–6863 (2013).
- 251 25. Ni, P. N. *et al.* Fabry-Perot resonance enhanced electrically pumped random lasing from ZnO films.

- 252 *Appl. Phys. Lett.* **107**, 231108 (2015).
- 253 26. Liu, X.-Y., Shan, C.-X., Wang, S.-P., Zhang, Z.-Z. & Shen, D.-Z. Electrically pumped random lasers
254 fabricated from ZnO nanowire arrays. *Nanoscale* **4**, 2843 (2012).
- 255 27. Yu, S. F. Electrically pumped random lasers. *J. Phys. D. Appl. Phys.* **48**, 483001 (2015).
- 256 28. Chu, S., Olmedo, M., Yang, Z., Kong, J. & Liu, J. Electrically pumped ultraviolet ZnO diode lasers on Si.
257 *Appl. Phys. Lett.* **93**, 181106 (2008).
- 258 29. Ma, X., Chen, P., Li, D., Zhang, Y. & Yang, D. Electrically pumped ZnO film ultraviolet random lasers on
259 silicon substrate. *Appl. Phys. Lett.* **91**, 251109 (2007).
- 260 30. Ma, X., Li, Y. & Yang, D. Electrically pumped random laser device based on dual SiO₂-ZnO structure and
261 preparation method and application thereof. (2012).
- 262 31. Qiao, Q. *et al.* Surface plasmon enhanced electrically pumped random lasers. *Nanoscale* **5**, 513–517
263 (2013).
- 264 32. Poison, R. C., Raikh, M. E. & Vardeny, Z. V. Universal properties of random lasers. *IEEE J. Sel. Top.*
265 *Quantum Electron.* **9**, 120–123 (2003).
- 266 33. Frolov, S. V, Vardeny, Z. V, Yoshino, K., Zakhidov, A. & Baughman, R. H. *Stimulated emission in high-*
267 *gain organic media.*

268

269 **Acknowledgements**

270 We gratefully acknowledge Stefano Caporali for his assistance with sputter deposition of Fabry-Perot mirrors
271 and Luca Mariani for advice on the optical fibre elements. We acknowledge Marco De Pas, Alessandro Montori
272 and Mauro Giuntini for their assistance in the set-up of electronics and Riccardo Ballerini and Ahmed Hajeb for
273 the realizations of mechanical elements.

274 This research was funded by Ente Cassa di Risparmio Firenze (2016-0866), Ministero dell'Istruzione
275 dell'Università e della Ricerca Italiano (PRIN2017-2017Z55KCW), European Community by Laserlab-Europe
276 (H2020 EC-GA-654148) and PATHOS EU H2020 FET-OPEN grant no. 828946.

277

278 **Contributions**

279 A.B, A.T, P.B, L.P, A.K.T, R.T and D.W conceived the experiment, A.B., A.T. and P.B. conducted the experiment
280 and analysed the results. A.B, A.T, L.P, A.K.T, R.T and D.W wrote the main manuscript text and A.B. prepared

281 the figures. All authors reviewed the manuscript.

282

283 **Corresponding author**

284 Correspondence to Diederik S. Wiersma and Alice Boschetti.

285

286 **Competing Interest**

287 The experimental apparatus and the analysis method are currently under patent filing.

288

289

290

Figure 1

291 Numerical demonstration of super-resolved spectroscopy.

292 a) A light source (broadband source or random laser) is used to illuminate a test sample (here a Fabry-Perot

293 (FP)), its transmission spectrum being measured using a spectrometer (S) with a large point spread function

294 (inset) and a linear camera (C). The numerical transmission function of the low finesse FP approximates a

295 sinusoid with a free spectral range of 125 GHz.

296 b) Average of 10^4 numerical broadband transmission spectra of the Fabry-Perot test sample. The target

297 transmission function is almost completely hidden by noise fluctuations and convolution with the broad

298 instrumental response.

299 c) Spectral reconstruction obtained by direct deconvolution of the average broadband spectrum using the

300 exact point spread function of the spectrometer (inset of panel a). The target response function is indicated by

301 a grey line (as measured by the camera with a spectral resolution of $\text{FWHM}=4.9\cdot\text{FSR}$). Deconvolution fails to

302 retrieve the original response, showing spurious amplitude modulations and high-frequency oscillations.

303 d) Exemplary set of simulated transmission spectra obtained by illuminating the sample with single random

304 laser shots, as measured by the low-resolution setup (blue). The original illumination spectra (dark blue)

305 exhibit narrow lasing lines over the active medium fluorescence curve.

306 e) Spectral reconstruction obtained using the method introduced in this paper, using 10^4 single shot random

307 laser spectra. On average, the original contrast of the Fabry-Perot is correctly restored, as well as its free

308 spectral range.

309

310
311
312
313
314
315
316
317
318
319
320
321
322
323
324
325
326
327
328
329
330
331
332
333
334
335
336
337
338

Figure 2

Experimental apparatus for super-resolved spectroscopy.

a) The random laser source (RL) is optically excited by a pulsed pump laser (LS) focused using a 10x microscope objective. The same objective collimates the backscattered signal while an interference filter blocks back-reflected pump light. A 50:50 beam splitter (BS) sends a reference signal to a first multimode fibre, while the probe passes through the sample (in this case a Fabry-Perot filter (FP)) before being focused to a second fibre. The two fibre cores are bundled together and simultaneously focused at the entrance of the spectrometer (S) so that their output can be collected by the same detector (C).

b) Illustrative single-shot emission spectrum from the random laser source characterized independently with high spectral resolution.

c) Transmission curve of the investigated Fabry-Perot sample, as measured independently using a high-resolution spectrometer and a broadband lamp.

d) Illustrative random laser single-shot measured with the experimental scheme of the panel (a) using a low resolution spectrometer. The transmission spectrum (cyan curve) is compared to its respective reference spectrum (light blue curve). Inset shows the measured instrumental response of the low-resolution spectrometer.

Figure 3

Low-resolution peak selection.

Exemplary low-resolution spectra measured by the CMOS camera under random laser illumination. The top and bottom rows in each frame correspond to the reference and transmitted signal, respectively. An algorithm finds the most intense, non-overlapping circles within a fixed diameter range.

Each shot allows to reconstruct a few points of the target function.

339

Figure 4

340

Experimental demonstration of super-resolved spectroscopy.

341

a) Transmission curve obtained by sparse sampling using the random laser. The target transmission function is

342

well reproduced exhibiting both its high- and low-frequency modulations, including its slow background slope

343

(cfr. Fig. 2c).

344

b) Transmission curve as obtained with a common lamp for comparison. As expected, the transmission

345

function of the Fabry-Perot etalon is lost due to convolution with the instrumental response function. c-d)

346

Fourier transform of a-b), showing a prominent peak corresponding to the inverse of the etalon free spectral

347

range, which is only visible in the case of our frequency-sparse sampling approach.

348

349

350

Methods

351

Random laser

352

A random laser is typically composed of a gain medium mixed with nanoparticles acting as scattering

353

elements. In a random laser there is no optical cavity in the traditional sense and the feedback mechanism

354

needed for lasing is provided by multiple scattering. Due to the disordered arrangement of the scattering

355

medium, laser emission from a random laser is typically characterized by very complex spectral features.

356

Few technical points need to be considered in order to achieve super-resolved spectral measurements.

357

First, the random laser source should exhibit, on average, a suitable distribution of chaotic lasing modes with

358

few intense peaks sparsely distributed with uniform probability over the emission spectrum. Secondly, the

359

emission spectrum of each lasing shot should be uncorrelated to the other shots (chaotic regime of operation).

360

These requirements can be easily fulfilled by adjusting the pump energy and the excitation volume,

361

representing a common mode of operation of a random laser.

362

In particular, varying the excitation volume allows to tune the average number of modes that go above

363

threshold at each pump event³²⁻³³, with a smaller volume (i.e., tighter pump lasing focusing) corresponding to

364 a sparser population of peaks over the gain bandwidth. The number of peaks should be such that the chance
365 of observing two overlapping peaks can be neglected.

366 The random laser sample is made of a colloidal suspension of ZnO nanoparticles (10^{12} particles per cm^3 ,
367 average particle diameter 200 nm) in a 5 mM solution of Rhodamine 6G dissolved in ethanol. The gain medium
368 is optically pumped with a frequency-doubled pulsed Nd:YAG laser system (Ekspla, Mod. PL2143A), emitting
369 pulses at 532 nm wavelength with a duration of 20 ps and a repetition rate of 10 Hz. We have determined for
370 this system a random lasing threshold of about $0.5\mu\text{J}$ per pulse, based on mode competition and gain
371 depletion. The chaotic lasing regime, characterized by shot-to-shot uncorrelated, narrow lasing modes, is
372 obtained for a pumping condition just above threshold¹⁷.

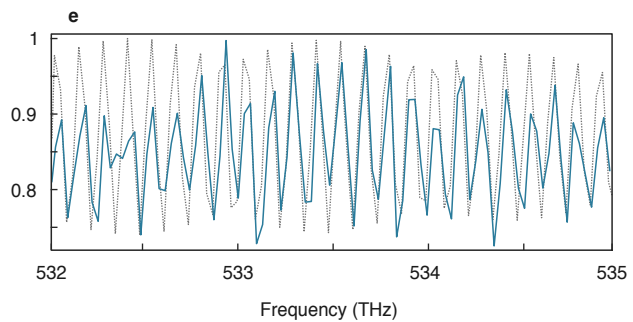
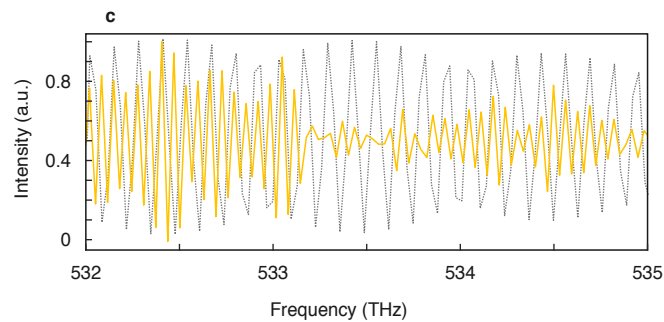
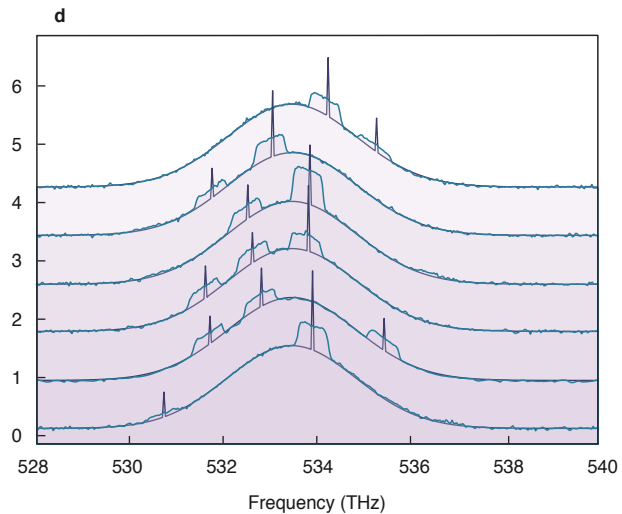
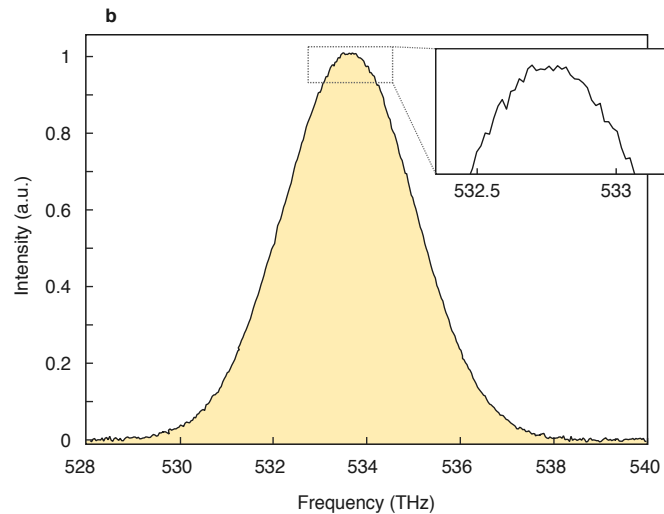
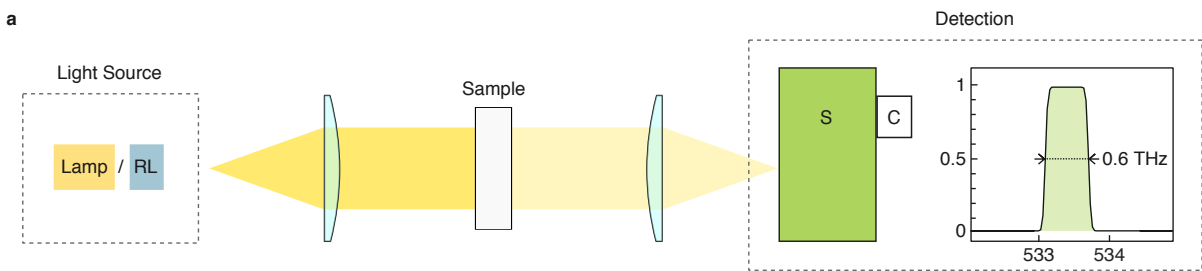
373 **Test sample**

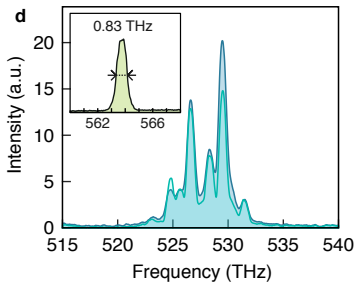
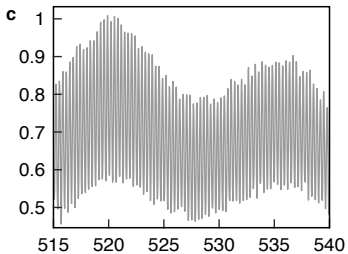
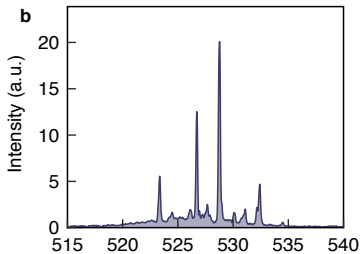
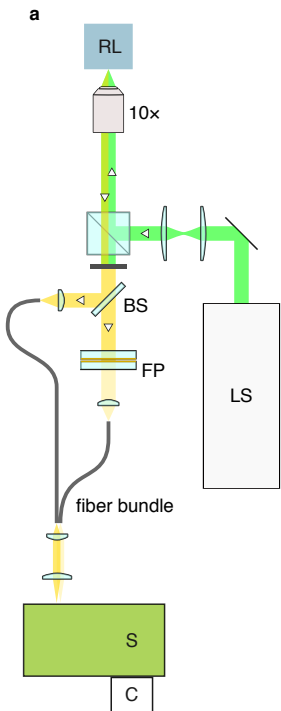
374 The low finesse Fabry-Perot (FP) test sample has been fabricated by sputter-coating a few nm of gold on
375 the uncoated facets of two IR flat mirrors, resulting in a reflectivity of about 30%. The distance between the
376 two mirrors was set so to obtain a free spectral range of 0.3 THz, corresponding to the finest FP modulation,
377 optically characterized with a higher resolution monochromator (Chromex, mod. 250 is entrance slit of 20 μm ,
378 600 grooves/mm grating) coupled to a digital camera (Thorlabs, mod. DCC1240C, 1280 \times 1024 pixel, 5.3 μm
379 pixel size). The maximum transmission contrast through the custom-made etalon, $(I_{\text{max}}-I_{\text{min}})/I_{\text{max}}$, is equal to
380 32% as measured using the incandescent lamp.

381 **Experimental setup**

382 The experimental set-up is shown schematically in Figure 2. The pump beam is collimated to a diameter of
383 8 mm to match the entrance pupil of a 10 \times microscope objective (NA 0.3, effective focal length 18 mm). The
384 objective focuses the pump beam to a 3 μm spot size on the surface of the random laser sample. The same
385 objective collects the random laser emission which is then divided using a beam splitter into a reference beam
386 and a probe beam. The reference is directly focused by a lens ($f=50$ mm) into one of the two entrances of a
387 multimodal fibre bundle (fibre diameters 50 μm). The probe beam passes through the test sample and is then
388 focused by a lens ($f=50$ mm) at the other fibre entrance. The two fibre outputs (separated by 85 μm) are
389 focused on the entrance slit of the monochromator and collected by the digital camera, synchronized with the
390 pump pulse. The resolution of the spectrometer can be tuned from an instrumental response of FWHM=0.13

391 THz to 0.83 THz by changing the input slit aperture from 20 μm to completely open. In the latter case, the
392 actual resolution is determined by the fibre output size (50 μm) and the entrance optics (3 \times magnification),
393 resulting in an effective illuminated aperture of 150 μm at the focal plane of the monochromator. This FWHM
394 corresponds to 2.8-FSR, and it is not sufficient to spectrally resolve the transmission function of the Fabry-
395 Perot test sample. The latter configuration has been used to demonstrate our super-resolution method and
396 reconstruct the transmission function of the test sample using the random laser source.
397





target diameter



reference



transmitted



